

Article

Flushing Capacity of a Stored Volume of Water: An Experimental Study

Sebastián Guillén-Ludeña ^{1,*} , Jorge A. Toapaxi ^{1,2}  and Luis G. Castillo ¹ 

¹ Hidr@m Research Group, Department of Mining and Civil Engineering, Universidad Politécnica de Cartagena, 30203 Cartagena, Spain

² Department of Civil and Environmental Engineering, Escuela Politécnica Nacional, Quito 170143, Ecuador

* Correspondence: sebastian.guillen@upct.es

Abstract: This paper presents a systematic analysis of the hydraulic flushing capacity of a stored volume of water to remove sediments. This analysis is based on 90 laboratory experiments in which the volume of sediment evacuated was measured for varying initial volumes of water, three bed slopes, and three sediment sizes. The experiments consisted of the rapid emptying of a reservoir by means of suddenly opening a tilting gate downstream. This opening produced an accelerated flow which eroded the mobile bed of the reservoir. The efficacy of flushing, herein defined as the ratio of the volume of sediments evacuated to the volume of water released, increased with the initial slope, and decreased as the initial volume of water increased. In relation to the sediment size, while the results obtained for the coarse and medium sands were very similar to each other, the results obtained for the fine sand were affected by the existence of apparent cohesion in the mobile bed. In comparison to the results obtained for the medium and coarse sands, this apparent cohesion reduced the volume of sediment evacuated by a given volume of water and hence, the efficacy of flushing.

Keywords: reservoir sedimentation; flushing efficacy; sediment transport; sedimentology; hydraulics



Citation: Guillén-Ludeña, S.; Toapaxi, J.A.; Castillo, L.G. Flushing Capacity of a Stored Volume of Water: An Experimental Study. *Water* **2022**, *14*, 2607. <https://doi.org/10.3390/w14172607>

Academic Editors: Sanjay Giri and Biswa Bhattacharya

Received: 24 July 2022

Accepted: 19 August 2022

Published: 24 August 2022

Publisher's Note: MDPI stays neutral with regard to jurisdictional claims in published maps and institutional affiliations.



Copyright: © 2022 by the authors. Licensee MDPI, Basel, Switzerland. This article is an open access article distributed under the terms and conditions of the Creative Commons Attribution (CC BY) license (<https://creativecommons.org/licenses/by/4.0/>).

1. Introduction

Reservoir sedimentation has become a major concern for dams' operators and owners. The gradual and incessant loss of storage capacity in reservoirs, owing to sediment deposition, reduces their operability and sustainability. In addition, the impoundment of sediments upstream of the dam alters the riverine sediment balance, resulting in a lack of sediments downstream [1,2]. This, in turn, leads to bed erosion and impoverished habitats downstream, owing to a deficit in those nutrients transported with the sediment particles [1,3]. In addition, the dam impedes the natural migration of riverine species upstream, which often results in a reduction in the species richness and the number of some assemblages [4]. In extreme cases, the sediment deposits in reservoirs may partially or totally block the water release structures, or even render the reservoir definitively inoperable [5,6]. The worldwide average loss of storage capacity has been estimated to range from 0.5% to 1.0% of volume per year [2,6–8]. Nevertheless, and depending on the region, this rate may reach higher values, such as the 4.3% reported by [9] for the reservoirs of California State in 2008. At a global scale, the loss of storage capacity owing to reservoir sedimentation, and the decrease in the rate at which new reservoirs are being built, have led to a decrease in the total net reservoir storage volume since 2000, and a decrease in the storage volume per capita since 1980 [1]. Moreover, these trends may be aggravated by a climate change scenario in which sediment yield is expected to increase [10,11], thereby raising the amounts of sediment being deposited in reservoirs.

Sediment management strategies seek to mitigate the negative effects derived from sediment depositing in reservoirs. Such strategies can be classified into three groups: (i) measures to reduce the fraction of sediment yield that enters the reservoirs; (ii) measures

to minimize sediment deposition within reservoirs; and (iii) measures to recover or to increase storage volume in the reservoir [2,12,13]. Among the measures included in the third group, the present study focuses on hydraulic flushing, which consists of the opening of the low-level outlets of a dam to remove previously deposited sediments. In addition, extreme cases of flushing are those dam removal projects in which the reservoirs are rapidly drawn down by breaching the dam [14–16]. Flushing has been reported as being one of the most efficient techniques for removing sediments from a reservoir [2,17,18]. However, this efficiency depends on factors such as the initial water level, the geometry of the reservoir, the capacity of the low-level outlets, the hydrology of the region, and the characteristics of the sediment deposited. Thus, when flushing is carried out with a water level that is so high as to cause a pressure flow through the low-level outlets, it is called pressure flushing, and the resulting erosion is limited to a cone-shaped zone in the vicinity of the outlets [19]. On the contrary, when the water level drops and the flow becomes a free-surface flow, it is called free-flow flushing, and the resulting erosion may extend several kilometers upstream of the outlets, eroding a channel and removing a large volume of sediments from the reservoir. Those reservoirs equipped with low-level outlets with a relatively large capacity, located in narrow valleys with steep sides, steep longitudinal slopes, and with strong seasonal flow patterns are the most suitable for successful flushing [2,13,17]. Additionally, [12] stated that, for flushing to be successful, the ratio of capacity to mean annual flow of the reservoir should be less than 4%, because a larger capacity would affect the reservoir draw down. Furthermore, periodic and controlled release of sediments from a reservoir can be beneficial for the riverine ecosystem, as it reduces the deficit of sediments downstream of the dam and may provide spawning grounds for fishes, especially when gravel predominates among the released sediments. On the contrary, when fine sediments are predominant in the release, severe environmental impacts can be created downstream of the dam. Flushing releases with fine sediments are characterized by high sediment concentrations and, consequently, they reduce the oxygen concentration, the visibility, and the light penetration. The deposition of sediment also often results in infilled pools and bed clogging, reducing the sites for spawning and impoverishing fish habitats [1].

The existing knowledge about flushing has been gained mainly from case studies based on field observations and measurements, performed during flushing operations in real reservoirs [2,3,13,17,18]. In addition, numerical studies, also based on case studies, have significantly contributed to characterizing and optimizing the processes involved in flushing [20–23]. In contrast, few experimental studies conducted under controlled laboratory conditions have systematically investigated the flushing technique. This is the case of the studies by [14], which focused on the geomorphic response of a channel after a dam removal, and that by [24], which focused on the evolution and characterization of the flushing channel and on the amount of sediment removed. Furthermore, in most of the flushing operations documented by the studies referred to above, sediments were eroded by the natural discharge of the river, which flowed through the low-level outlets as a free-surface flow. In this context, the present study focuses on those reservoirs located in arid or semiarid regions in which the hydrological conditions result in weak river discharges with low or negligible erosion capacity for flushing. Thus, the available water for flushing is that previously stored in the reservoir.

Therefore, the present study proposes a detailed, novel, and systematic experimental approach with the following objectives:

- To analyze the capacity of flushing sediments in a reservoir using only that water previously stored in it.
- To characterize the effects of the initial water head, the initial volume of water, the bed slope, and the sediment grain size on the efficacy of flushing. This efficacy is herein defined as the volume of sediments removed to the volume of water released.

To address these objectives, 90 laboratory experiments were conducted at the hydraulic laboratory of Universidad Politécnica de Cartagena, Spain. These experiments included different configurations of the reservoir geometry, bed slope, and sediment grain size.

2. Methodology

2.1. Experimental Facility and Procedure

The experimental facility consisted of a 15 m long, 0.31 m wide, and 0.50 m high rectangular glass-wall flume, with an adjustable longitudinal slope. The flume was equipped with a sluice gate upstream, a tilting gate downstream, and a sediment trap at the downstream end of the flume. The tilting gate was the same width as the flume ($B = 0.31$ m) to characterize the maximum hydraulic capacity of the stored volume for flushing. The bottom was elevated 0.15 m along 6 m, to ensure supercritical flow downstream of the tilting gate. The origin of coordinates was located at the downstream end on the elevated bottom (Figure 1).

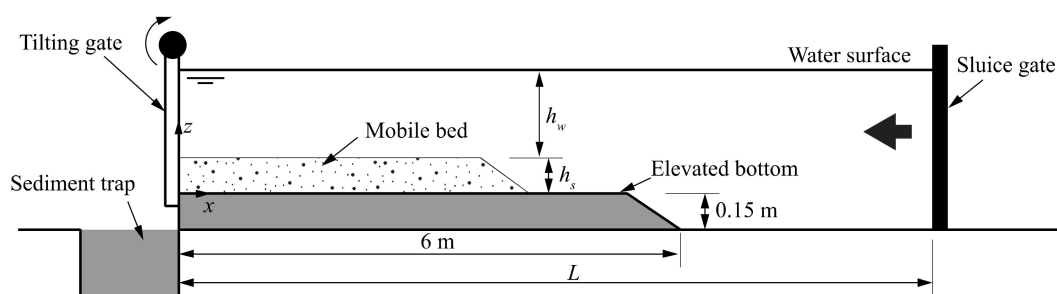


Figure 1. Sketch of the experimental facility. Not to scale.

Figure 1 sketches a lateral view of the experimental facility in which h_s stands for the initial thickness of the sediment layer, h_w is the initial water head measured from the top of the sediment layer, and L is the reservoir length, comprised between the tilting gate (downstream) and the sluice gate (upstream) (Figure 1). Both h_w and h_s varied from 0.05 m to 0.20 m by intervals of 0.05 m, and combined they gave ten pairs h_s-h_w , in which:

- For $h_s = 0.05$ m, $h_w = 0.05$ m, 0.10 m, 0.15 m, and 0.20 m.
- For $h_s = 0.10$ m, $h_w = 0.05$ m, 0.10 m, and 0.15 m.
- For $h_s = 0.15$ m, $h_w = 0.05$ m, and 0.10 m.
- For $h_s = 0.20$ m, $h_w = 0.05$ m.

The sediments consisted of three non-cohesive, well-sorted silica-sands ($\rho_s = 2600$ kg/m³) with $d_{50} = 0.39$, 0.80, and 1.54 mm, referred to as fine, medium, and coarse, respectively.

The experimental set-up consisted of a total of 90 experiments, including:

- Thirty experiments in which ten pairs h_s-h_w were tested for an initial bed slope $S_0 = 0.0\%$, for the medium sand, and for three different reservoir lengths: $L = 5.997$ m, 9.287 m, and 12.043 m with $\Delta L = \pm 0.001$ m accuracy.
- Twenty experiments in which ten pairs h_s-h_w were tested for $S_0 = 0.5\%$, and 1.0%, for the medium sand, and for $L = 12.043$ m.
- Forty experiments in which ten pairs h_s-h_w were tested for $S_0 = 0.0\%$, for the fine and coarse sands, and for $L = 5.997$ m, and 12.043 m.

Prior to each experiment, a layer of unconsolidated loose sediments of thickness h_s was extended and leveled throughout the elevated bottom with $\Delta h_s = \pm 0.003$ m accuracy. Later, the flume was carefully filled up with water until reaching the level h_w with $\Delta h_w = \pm 0.001$ m accuracy, and the upstream sluice gate was closed to confine the initial volume of water (V_w). The experiment started with a sudden opening of the tilting gate, and it finished when the initial volume of water (V_w) was completely evacuated from the flume, along with a volume of sediments (V_s). These sediments were collected in the sediment trap, to be reused in subsequent experiments. Once the experiment had finished, the abscise of the final position of the knickpoint x_s was measured with $\Delta x_s = \pm 0.005$ m accuracy (Figure 2). All the experiments were laterally recorded to follow the evolution of the bed and the water surface. Figure 2 shows a lateral view of the experimental facility just before the beginning

of one experiment and after finishing it. The final slope of the bed, downstream of the knickpoint, was computed as $S_f = h_s/x_s$ (Figure 2b), and V_s was estimated geometrically as:

$$V_s = \frac{1}{2} \cdot B \cdot h_s^2 \cdot \frac{1}{S_f} \tag{1}$$

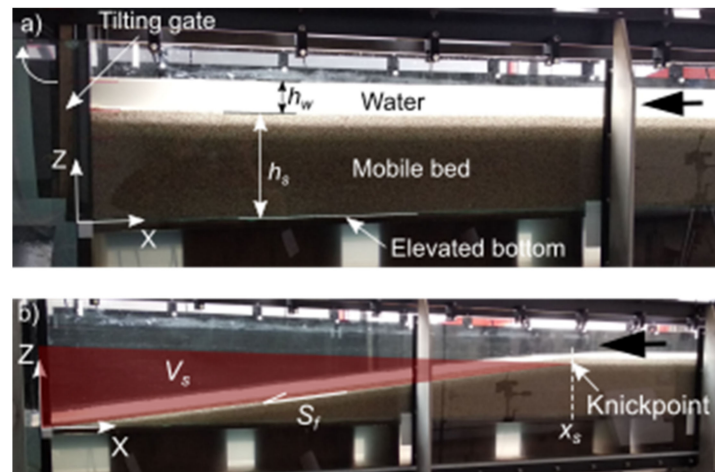


Figure 2. (a) Lateral view of the experimental facility just before the beginning of one experiment. (b) Lateral view of the experimental facility at the end of the experiment.

Thus, the steeper S_f , the lower V_s , and vice versa. The measurement errors of S_f and V_s were estimated as:

$$\Delta S_f = \frac{\Delta h_s \cdot x_s + h_s \cdot \Delta x_s}{x_s^2} \tag{2}$$

$$\Delta V_s = \frac{(\Delta B \cdot h_s^2 + B \cdot 2 \cdot h_s \cdot \Delta h_s) \cdot S_f + B \cdot h_s^2 \cdot \Delta S_f}{2 \cdot S_f^2} \tag{3}$$

where $\Delta B = \pm 0.005$ m.

2.2. Dimensional Analysis

A dimensional analysis was performed in order to characterize the effects of the reservoir geometry, the sediment characteristics, and the initial water head on S_f . Thus, S_f depends on the following variables:

$$S_f = f(B, L, h_w, h_s, S_0, d_{50}, \rho, \rho_s, \nu, g, u_{*cr}) \tag{4}$$

where, obviating those variables already defined, B is the width of the flume, ρ is the density of water, ν is the kinematic viscosity of water, g is the gravitational acceleration, and u_{*cr} is the critical shear velocity according to [25]. In this analysis, B can be eliminated because it remains constant for all the experiments. Thus, by considering h_s as the length scale, $\rho \cdot h_s^3$ as the mass scale, and h_s/u_{*cr} as the time scale, the Buckingham π theorem yields:

$$S_f = f\left(\frac{L}{h_s}, \frac{h_w}{h_s}, S_0, \frac{d_{50}}{h_s}, \frac{\rho_s - \rho}{\rho}, \frac{\nu}{u_{*cr} \cdot h_s}, \frac{g \cdot h_s}{u_{*cr}^2}\right) \tag{5}$$

which, rearranged, reads:

$$S_f = f\left(\frac{h_w \cdot L}{h_s^2}, S_0, \frac{\nu}{u_{*cr} \cdot d_{50}}, \frac{g \cdot d_{50}}{u_{*cr}^2} \cdot \frac{\rho_s - \rho}{\rho}\right) \tag{6}$$

which is equivalent to:

$$S_f = f\left(\frac{h_w \cdot L}{h_s^2}, S_0, Re^*, \tau^*_{-cr}\right) \tag{7}$$

where Re^* and τ^*_{-cr} are the Shields' parameters [25]. These parameters can be combined as $D^* = Re^{*2/3} \cdot \tau^*_{-cr}{}^{1/3}$, which is the non-dimensional sediment diameter [26]. Thus, the dimensional analysis finally yields:

$$S_f = f\left(\frac{h_w \cdot L}{h_s^2}, S_0, D^*\right) \tag{8}$$

where $h_w \cdot L/h_s^2$ is the product of the initial water head to sediment thickness ratio (h_w/h_s) and the reservoir length to sediment thickness ratio (L/h_s). The measurement error of the parameter $h_w \cdot L/h_s^2$ was estimated as:

$$\Delta \frac{h_w \cdot L}{h_s^2} = \frac{(\Delta h_w \cdot L + h_w \cdot \Delta L) \cdot h_s^2 + h_w \cdot L \cdot 2h_s \cdot \Delta h_s}{h_s^4} \tag{9}$$

This analysis is also valid for characterizing the flushing efficacy (V_s/V_w) as a function of the reservoir geometry, the sediment characteristics, and the initial water head. Thus, by expressing S_f as a function of V_s from Equation (1) and substituting in Equation (8), it reads:

$$\frac{\frac{1}{2} \cdot B \cdot h_s^2}{V_s} = f\left(\frac{h_w \cdot L}{h_s^2}, S_0, D^*\right) \tag{10}$$

where multiplying the term on the left side by h_w/h_s and by L/h_s , and multiplying the first parameter on the right side by B/h_s , it reads:

$$\frac{B \cdot h_w \cdot L}{V_s} = f\left(\frac{B \cdot L \cdot h_w}{h_s^3}, S_0, D^*\right) \tag{11}$$

which is equivalent to:

$$\frac{V_s}{V_w} = f\left(\frac{V_w}{h_s^3}, S_0, D^*\right) \tag{12}$$

where V_s/V_w stands for the efficacy of the flushing, and V_w/h_s^3 is the non-dimensional initial volume of water. Table 1 shows the values adopted in this study for the aforementioned governing parameters.

Table 1. Adopted values for the governing variables and parameters.

$h_w \cdot L/h_s^2$	V_w/h_s^3	S_0	D^*
[-]	[-]	[%]	[-]
Min = 7.5	Min = 11.5	0.0	10 (Fine)
Max = 963.4	Max = 5934.8	0.5%	20 (Medium)
		1.0%	39 (Coarse)

2.3. Studies for Comparison

The results obtained in this study have been compared to the results obtained from laboratory experiments by [24], and to the field measurements reported for the flushing operations of the Condit dam in USA [15], and the Gebidem dam in Switzerland [2]. Despite the existing differences between these previous studies and the experiments conducted in this study, mainly in terms of reservoir and outlet geometries and sediment characteristics, all these studies report on the rapid release of a previously stored volume of water, which provokes the erosion of the bed evacuating a volume of sediments. For comparison, the values of the variables L , h_w , h_s , V_w , V_s , and S_f were obtained for each of these previous studies, to compute the parameters $h_w \cdot L/h_s^2$ and V_w/h_s^3 . The effects of S_0 and D^* on the

final bed slope (S_f) and on the efficacy of flushing (V_s/V_w) were not analyzed for these studies, because the available data did not enable the individual effects of these variables on the overall process to be decoupled.

The experiments by [24] were conducted in a 50 m long, 2.4 m wide, horizontal and rectangular flume at the hydraulic laboratory of University of California at Berkeley (USA). In that flume, a reservoir was modeled within the upstream 30 m of the flume. The outlet consisted of a 0.15 m wide, 0.25 m high rectangular sluice gate, located at the downstream end of the reservoir. For each experiment, a 0.10 m thick and unconsolidated sediment layer was extended on an elevated bottom, approximately 9 m from the outlet. The sediment material consisted of walnut shell grit ($d_{50} = 1.25$ mm and $\rho_s = 1.39$ kg/m³). The reservoir was filled with water until the desired water level was reached. Then, the discharge was set to the desired value and the sluice gate was opened until the steady state was reached, i.e., constant water level and the outlet discharge equal to the incoming one. To start the experiments, the gate was opened at a constant rate of approximately 5 cm per minute, until the opening reached 10 cm above the elevated bottom. Each experiment lasted approximately 30 min, during which time the incoming discharge was kept constant, and the outlet hydrograph and solidograph were measured. In those experiments, different discharges ranging from 0.56 m³/s to 4.86 m³/s were tested. The initial water level (h_w) varied from 0.02 m to 0.07 m, measured from the top of the sediment layer. The data for those experiments were obtained directly from [27], with the exception of L and V_w . L was estimated as $V_w/(B \cdot h_w)$ for each run, where B was the width of the laboratory flume, i.e., 2.4 m, and V_w was computed from the corresponding liquid hydrograph.

The case of the Condit dam consisted of the removal of a 38 m-high dam on the White Salmon River (USA), which stored $1.8 \cdot 10^6$ m³ of sediments. Prior to the demolition of the dam, the reservoir was rapidly emptied by blasting a 5 m wide hole into the base of the dam. This blast led to a rapid reservoir draw down and to an abrupt release of water and sediments, which lasted approximately five hours [15]. During that time, a channel was eroded approximately 1 km from the dam. Although the erosion and the transport of sediment downstream of the dam continued for several weeks, it was provoked by the natural discharge of the river, rather than by the water previously stored in the reservoir. Hence, in this study, only the first five hours after breaching were considered for comparison. Thus, L , h_w , h_s , and S_f were obtained directly from Figure 2 in [15]. h_s was estimated as the average difference between the pre-dam bathymetry and that performed in 2006, considering the nearest 1 km to the dam. S_f was estimated from the 56 days post-breach profile, by considering an average value for the nearest 1 km to the dam. V_s and V_w were calculated for the first five hours after the dam breaching from the sediment concentrations and discharge hydrograph, respectively (Figure 4 in [15]).

The third case considered for comparison in this study is that concerning the flushing operation conducted in the Gebidem dam in Switzerland, in 1991 [2]. This flushing operation began with the water level of the reservoir at its minimum operational level, at which the water surface extended some 450 m from the dam. Then, the low-level outlets were opened for 96 h, while the discharge hydrograph and suspended sediment concentrations were measured. The volume of water previously stored in the reservoir was released within the first two hours of flushing. After that, the natural river discharge flowed through the low-level outlets, carrying sediments downstream of the dam. In that study, only the first two hours of flushing were considered for comparison. In this case, L , h_w , h_s , and S_f were estimated from Figure 21.8 in [2], by considering the nearest 450 m to the dam. V_w and V_s were computed from the discharge hydrograph and the values of suspended solid concentrations shown in Figure 21.6 in [2]. Table 2 contains the values of the variables and parameters needed for comparison.

Table 2. Values for the variables and parameters obtained from previous studies for comparison.

Dam/Experiment	Data Source	L	h_w	h_s	V_w	V_s	S_f	$h_w \cdot L/h_s^2$	V_w/h_s^3	V_s/V_w
		[m]	[m]	[m]	[m ³]	[m ³]	[-]	[-]	[-]	[%]
Condit (USA)	[15]	2900	25	8	1.6×10^6	1.8×10^5	1.4%	1192	3354	12%
Gebidem (CH)	[2]	450	13	10	0.3×10^6	1.0×10^5	4.1%	62	292	38%
Lai and Shen Run 1		33	0.07	0.1	5.53	0.21	-	230	5530	4%
Lai and Shen Run 2		22	0.07	0.1	3.69	0.22	-	154	3691	6%
Lai and Shen Run 3		42	0.03	0.1	3.31	0.26	-	138	3313	8%
Lai and Shen Run 4	[27]	24	0.07	0.1	4.13	0.31	-	172	4134	7%
Lai and Shen Run 6		35	0.07	0.1	5.75	0.20	-	239	5747	3%
Lai and Shen Run 7		30	0.07	0.1	4.98	0.27	-	208	4982	5%
Lai and Shen Run 8		36	0.02	0.1	1.93	0.20	-	80	1930	10%

Other field and laboratory studies in which water and sediments were suddenly released by an abrupt dam removal were also analyzed for comparison, but they were discarded for different reasons. These are the cases of the removal of the Marmot dam [16], the failure of the Barlin dam [28], and the experiments by [14]. The case of the Marmot dam was discarded because the water stored in the reservoir prior to the dam breaching was mostly responsible for the erosion of the earth cofferdam, whereas the sediments impounded in the reservoir were mostly eroded by the natural discharge of the river. [16]. The abrupt failing of the Barlin dam in Japan during the typhoon WeiPa in 2007 was discarded for comparison, because no data of the volume of water previously stored in the reservoir were found [28]. The experiments by [14] were discarded because the outlet volumes of water and sediments were not reported for the experiments.

3. Results

3.1. Morphodynamics of the Experiments

Every experiment began with a sudden opening of the tilting gate, which provoked a steep hydraulic gradient, flow acceleration, and rapid vertical erosion of the sediment front. This erosion led to the formation of a knickpoint that migrated upstream as the sediment front was eroded (Figures 3 and 4). In this study, and according to [29], a knickpoint is that point at which the longitudinal slope of the bed changes abruptly (Figures 3 and 4). The migration of the knickpoint was fast during the first instants of the experiments, and it was associated with intense sediment transport. For the coarse and medium sands, the sediment front pivoted around the edge of the elevated bottom at the downstream end, and its gradient decreased as the knickpoint migrated upstream (Figure 3). Meanwhile, the flow discharge gradually decreased until the initial volume of water (V_w) was completely evacuated. At the instant at which the flow was not enough to entrain any more sediments, the knickpoint ceased its migration and the sediment front reached the final slope (S_f) (Figures 3E and 4F). In contrast, for the fine sand, the sediment front migrated upstream by keeping a roughly constant gradient, while downstream of the front, all sediments were transported by the flow (Figure 4D). This lasted until the transport capacity of the flow diminished and sediments began to deposit downstream of the sediment front. The deposited sediments and the sediment front merged gradually, creating a final bed surface with a uniform slope (S_f), similar to those observed for the coarse and medium sands (Figure 4E). Upstream of the knickpoint, no sediment transport was observed for any of the experiments. The aforementioned features are illustrated in Figures 3 and 4, which depict the evolution of the bed and water surfaces of two representative experiments at different instants. These experiments were performed for $h_w L/h_s^2 = 26.65$, $V_w/h_s^3 = 54.73$, $S_0 = 0.0\%$ and for medium and fine sands (Figures 3 and 4, respectively).

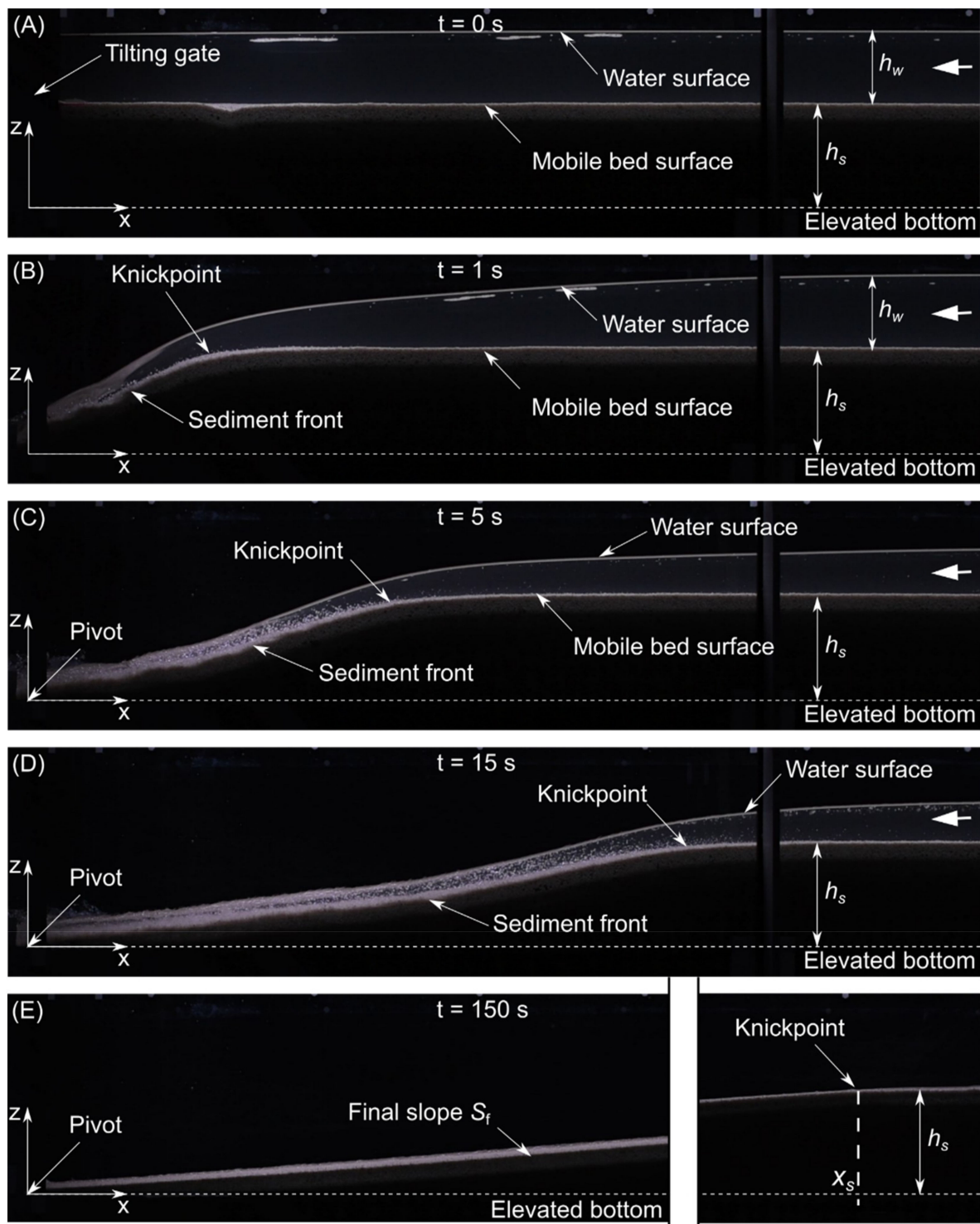


Figure 3. Lateral view of the experiment performed with medium sand, $h_w \cdot L/h_s^2 = 26.65$, $V_w/h_s^3 = 54.73$, and $S_0 = 0.0\%$ at the instants: (A) $t = 0$ s, (B) $t = 1$ s, (C) $t = 5$ s, (D) $t = 15$ s, and (E) $t = 150$ s.

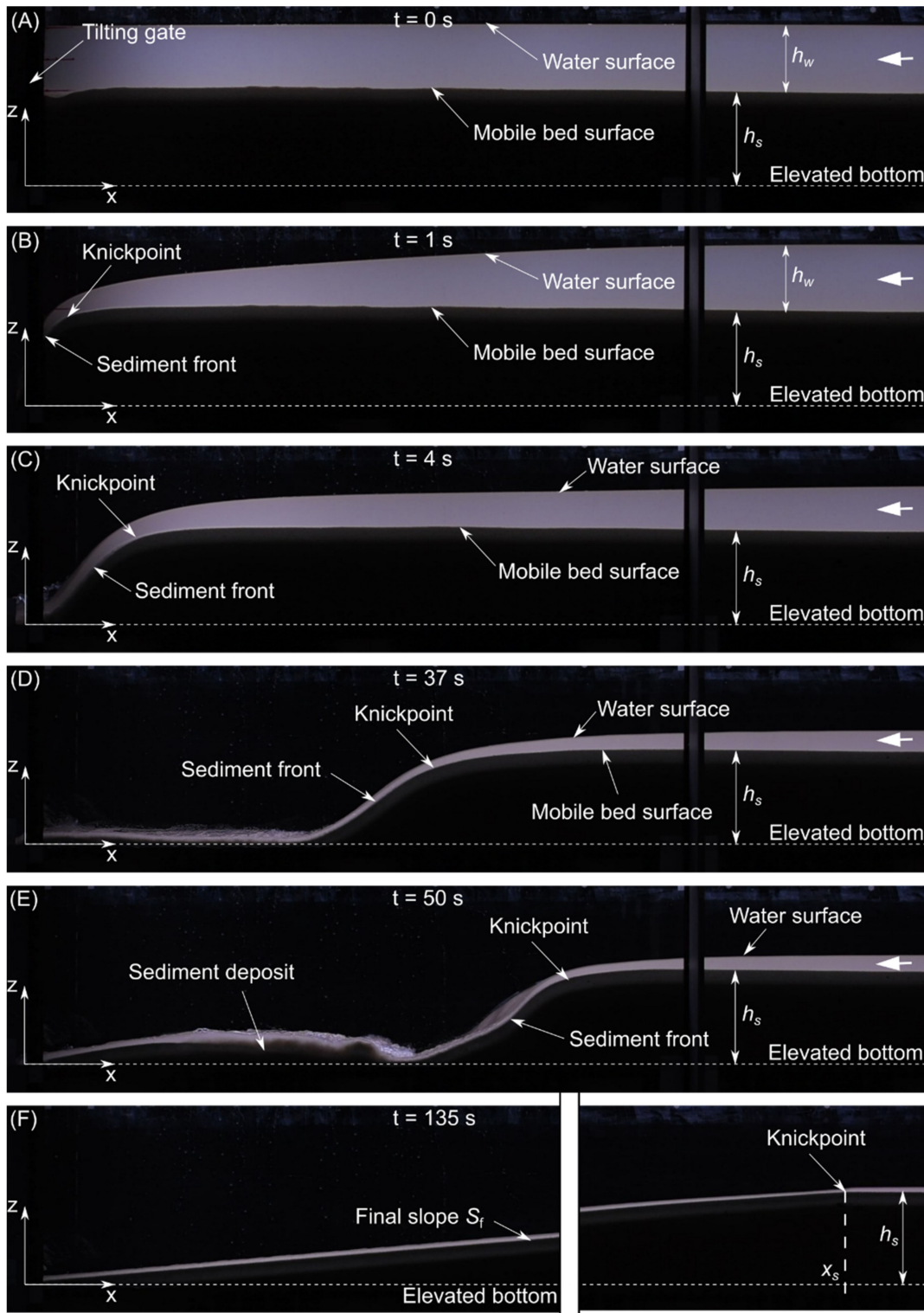


Figure 4. Longitudinal profiles of the bed surface and water surface for the experiment performed with fine sand, $h_w \cdot L/h_s^2 = 26.65$, $V_w/h_s^3 = 54.73$, and $S_0 = 0.0\%$ at the instants: (A) $t = 0$ s, (B) $t = 1$ s, (C) $t = 4$ s, (D) $t = 37$ s, (E) $t = 50$ s, and (F) $t = 135$ s.

3.2. S_f for Varying Values of $h_w \cdot L/h_s^2$, D^* , and S_0

Figure 5a shows the evolution of S_f for the experiments performed for $S_0 = 0.0\%$, and for varying values of $h_w \cdot L/h_s^2$, and D^* . In this experimental setup, the relative error $\Delta S_f/S_f$ varies from 2% to 7%, with an average value of 4%, and $\Delta (h_w \cdot L/h_s^2)/h_w \cdot L/h_s^2$ varies from

5% to 14%, with an average value of 9%. For the sake of clarity, error bars are not shown in the figure. Additionally, the values of S_f and $h_w \cdot L / h_s^2$ obtained for the flushing operations of the Gebidem and Condit dams are illustrated in Figure 5a. In this study, S_f was observed to decrease as the ratios h_w / h_s and L / h_s increased individually (not shown). Hence, it is assumed that the evolution of S_f for varying values of $h_w \cdot L / h_s^2$ is also representative of the individual effects of h_w / h_s and L / h_s on S_f . In these experiments, S_f decreased as the value of $h_w \cdot L / h_s^2$ increased. Namely, S_f ranged from 0.21 for $h_w \cdot L / h_s^2 = 13$ to 0.03 for $h_w \cdot L / h_s^2 = 963$. This trend was also observed when comparing the values obtained for the Gebidem and Condit dams, although the values of S_f obtained in this study were higher than those reported for the dams. In the present study, the values of S_f obtained for the coarse and medium sands were very similar, but they differed from those values obtained for the fine sand. Namely, for $h_w \cdot L / h_s^2 < 134$ approximately, the values of S_f obtained for the coarse and medium sands were lower than those obtained for the fine sand, whereas for $h_w \cdot L / h_s^2 > 134$ and for the coarse and medium sands, S_f was steeper than for the fine sand. In some experiments, there were different values of S_f measured for the same value of $h_w \cdot L / h_s^2$. These were the cases in which, for a given value of h_s , different values of h_w and L led to the same value for the product $h_w \cdot L$. For instance, for $h_s = 0.05$ m, those configurations in which $h_w = 0.05$ m— $L = 12.043$ m and $h_w = 0.10$ m— $L = 5.997$ m, both resulted in $h_w \cdot L / h_s^2 = 240$. In those cases, S_f increased as the ratio h_w / L decreased, where h_w / L denotes the initial hydraulic gradient of the reservoir. Regarding S_0 , the steeper it was, the steeper the S_f was. Nevertheless, it is important to note that, for given values of h_w and L , V_w decreased as S_0 increased. Hence, when comparing values of S_f measured for different values of S_0 , one must take into account that the initial volume of water (V_w) was also different. Therefore, the increase in S_f and the respective decrease in V_s must be attributed to the decrease in V_w , rather than to the increase in S_0 . Figure 5b shows the evolution of S_f for the experiments performed with medium sand, and for varying values of $h_w \cdot L / h_s^2$, and S_0 . In terms of the volume of sediment evacuated (V_s) and according to Equation (1), V_s increased as $h_w \cdot L / h_s^2$ and S_0 increased. Regarding D^* , for $h_w \cdot L / h_s^2 < 134$ the value of V_s was larger for the coarse and medium sands than for the fine sand, whereas for $h_w \cdot L / h_s^2 > 134$, the values of V_s obtained for the fine sand were larger than those obtained for the coarse and medium sands. Moreover, for a given value of h_s and for a given value of $h_w \cdot L$, V_s was larger in those configurations with relatively low hydraulic gradients (h_w / L).

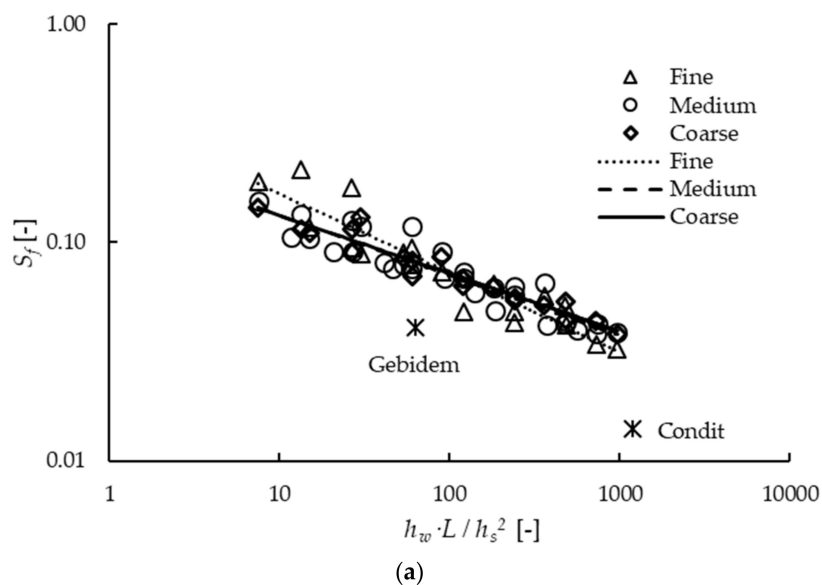


Figure 5. Cont.

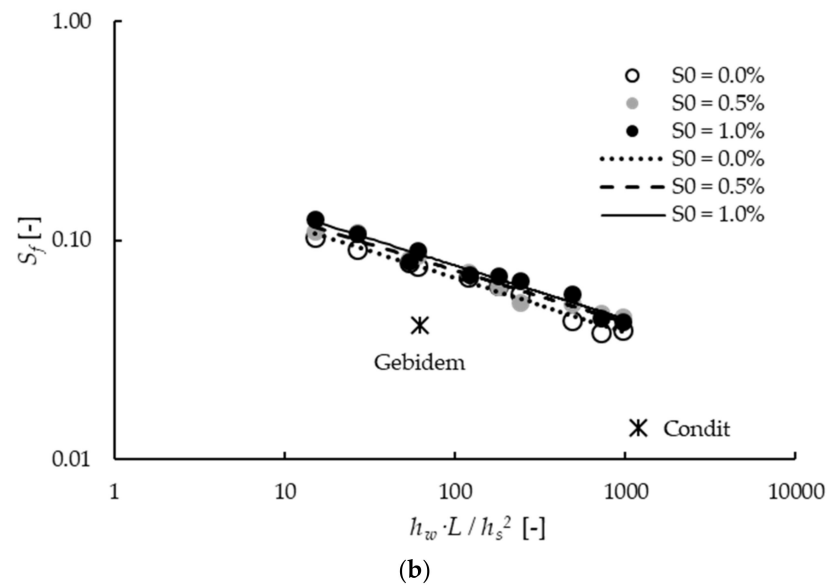


Figure 5. (a) Evolution of S_f for $S_0 = 0.0\%$ and for varying values of $h_w \cdot L / h_s^2$ and D^* . (b) Evolution of S_f for medium sand and for varying values of $h_w \cdot L / h_s^2$ and S_0 .

3.3. Flushing Efficacy for Varying Values of V_w/h_s^3 , S_0 and D^*

The evolution of the flushing efficacy (V_s/V_w) for varying values of V_w/h_s^3 , S_0 and D^* is illustrated in Figure 6, along with the values of V_w/h_s^3 and V_s/V_w corresponding to the flushing operations of the Gebidem dam [2], the Condit dam [15], and those corresponding to the experiments performed by [24]. The results of this study show that V_s/V_w decreased as V_w/h_s^3 increased, for the three values of S_0 and for the three values of D^* . Namely, V_s/V_w varied from 0.63 for $V_w/h_s^3 = 11$ to 0.01 for $V_w/h_s^3 = 79$. The values of V_s/V_w obtained for the Gebidem and Condit dams, and for the experiments by [24], also decreased as V_w/h_s^3 increased. However, for a given value of V_w/h_s^3 , the values of V_s/V_w measured in this study were lower than those obtained for the Gebidem and Condit dams and for the experiments by [24] (Figure 6). In this study, for the fine sand, the values of V_s/V_w measured for $V_w/h_s^3 < 100$ were lower than those measured for the coarse and medium sands. For those experiments with the same value of V_w/h_s^3 but different values for h_w and L , the flushing efficacy increased as the ratio h_w/L decreased (not shown). Regarding S_0 , the steeper it was, the higher the flushing efficacy (V_s/V_w) was. This pattern is highlighted in Figure 6 by means of three trend lines corresponding to each value of S_0 . These lines were obtained by means of Equation (13) (see below) for each value of S_0 . Equation (13) characterizes the influences of V_w/h_s^3 , S_0 and D^* on V_s/V_w as:

$$\frac{V_s}{V_w} = (0.745 + 88.250 \cdot S_0 + 0.041 \cdot D^*) \cdot \left(\frac{V_w}{h_s^3}\right)^{-(0.417 + 4.320 \cdot S_0 + 0.005 \cdot D^*)} \tag{13}$$

where the coefficients were calculated by means of the least square method, in order to obtain the best fitting curve for the whole dataset. Thus, Equation (13) provides the value of V_s/V_w as a function of V_w/h_s^3 , S_0 and D^* ; with an average relative error of $\pm 17\%$ regarding the values measured in the experiments. Figure 7 depicts the correlation between the values of V_s/V_w obtained from the experiments and those obtained by means of Equation (13), along with the error lines corresponding to $\pm 17\%$.

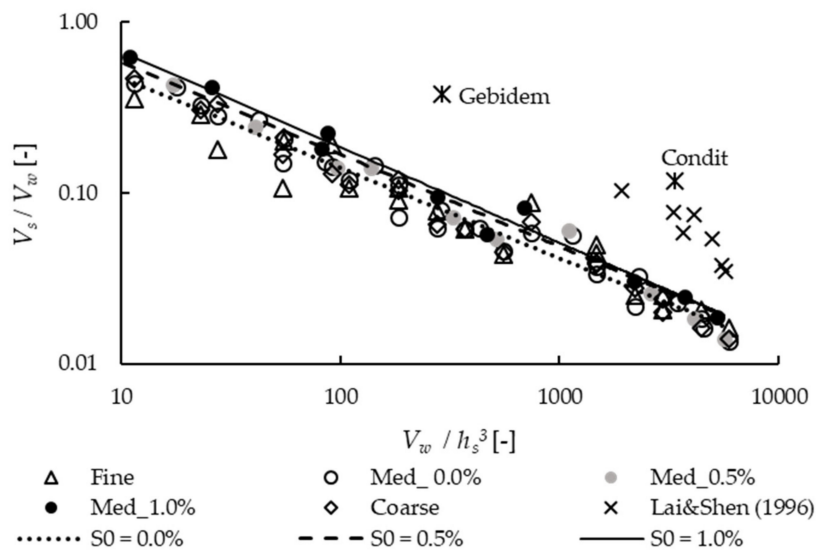


Figure 6. Evolution of V_s/V_w for varying values of V_w/h_s^3 , S_0 , and D^* .

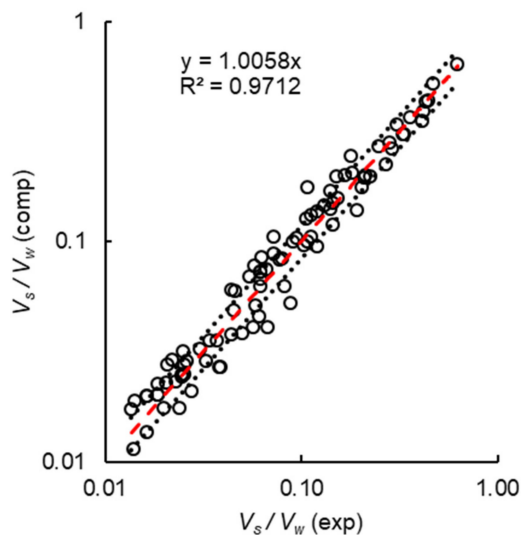


Figure 7. Correlation between the values of V_s/V_w obtained from the experiments and those computed with Equation (13). Dotted lines correspond to a relative error of $\pm 17\%$.

4. Discussion

The experiments conducted in this study characterize the capacity of a stored volume of water to erode a mobile bed by means of flushing. The efficacy of the flushing (V_s/V_w) was evaluated for different initial conditions (h_w, h_s, V_w, S_0) and for different sediment sizes (D^*). During the experiments, the evolution of the bed morphology was characterized by: (i) an initial rapid and short vertical incision in the mobile bed that led to the formation of a knickpoint, (ii) a rapid upstream migration of it, accompanied by an intense sediment transport, retrogressive erosion, and bed degradation downstream of the knickpoint; and (iii) a slowdown of the knickpoint migration and a decrease in the sediment transport rate, downstream of the knickpoint. Finally, the bed profile was shaped by a roughly uniform slope (S_f) downstream of the knickpoint, and by an unaltered horizontal surface upstream of it (Figures 3E and 4F). Similar patterns for the bed morphology are commonly observed in nature in those channels with a base-level lowering downstream, although the time scale of the process may vary significantly, depending on the case [15,16,28–35]. In nature, a base-level lowering leading to a knickpoint migration may originate either

from natural processes [32], or from human interventions such as reservoir flushing or dam removals [2,15,16,35–37]. Typically, the upstream migration of the knickpoint is associated firstly with a rapid incision of the bed, and secondly with a slower widening of the incised channel. Initially, the incised channel may undergo narrowing, depending on the flow discharge [14]. In these experiments, bed erosion was uniform across the channel width, and hence, neither narrowing incision nor widening of it were observed. The absence of narrowing incision during the initial stage of the experiments can be attributed to the high flow discharge, resulting from both the sudden opening and the width of the outlet. The absence of channel widening can be attributed, on the one hand, to the full-width uniform erosion registered from the beginning of the experiments and, on the other hand, to the rigid lateral banks that impeded lateral erosion. The stages observed during the evolution of these experiments are analogous to those reported by [34], who characterized the channel response to dam removal by a conceptual model, including six stages. In this study, all the stages reported by [34] were registered, with the exception of stage D, which corresponds to channel widening. Stage B, in which the bed remains unaltered while the water level is lowering, was observed only upstream of the knickpoint, whereas downstream, stage C (degradation) followed stage A (pre-removal). Stage E, which characterizes bed aggradation downstream, was observed only for the experiments performed with fine sand (Figure 4E). Finally, the equilibrium of the bed (stage F) was reached when the flow discharge diminished and no more sediments were transported. Similar bed evolution, albeit with lateral erosion, was reported for the laboratory experiments by [14,24], and for the field observation during the removal of the Marmot and Condit dams in the USA [15,16], and after the failure of the Barlin dam in Japan [28].

The final bed slope registered downstream of the knickpoint (S_f) was observed to decrease as the value of $h_w \cdot L / h_s^2$ increased (Figure 5). Thus, the larger the initial volume of water per unit width ($h_w \cdot L$) was with respect to the thickness of sediments (h_s), the lower S_f was and, consequently, the larger the volume of sediment evacuated (V_s) was. This pattern was also observed for the data reported for the flushing operations conducted at the Gebidem and Condit dams ([2] and [14], respectively) (Figure 5). Moreover, the lower values of S_f observed for those two dams with respect to the values obtained in this study are, presumably, owing to the lateral erosion. In these dams, the lateral erosion contributed to flattening the bed slope by bringing sediments into the incised channel.

In these experiments, S_f and, consequently, V_s were influenced by the sediment size, herein characterized by D^* . The evolution of the experiments performed with fine sand and the results obtained from them differ from those obtained for the coarse and medium sands. These differences can be attributed to the existence of apparent cohesion in those mobile beds prepared with fine sand. These beds were not fully saturated owing to the unavoidable pores filled with air and confined within the soil matrix. Apparent cohesion is typically observed in unsaturated granular soils, as a result of negative pressures exerted by capillary forces within the soil matrix [38,39]. During the upstream migration of the knickpoint, this cohesion led to steep and roughly constant slopes of the sediment front [30]. This contrasts with the gradually decreasing and comparatively mild slope observed for the coarse and medium sands (Figures 3 and 4). In addition, for the fine sand, the effect of the apparent cohesion was enhanced as h_s increased and, consequently, $h_w \cdot L / h_s^2$ decreased. This resulted in comparatively high values of S_f for $h_w \cdot L / h_s^2 < 134$, with respect to the values of S_f measured for the coarse and medium sands. On the contrary, for relatively low values of h_s ($h_w \cdot L / h_s^2 > 134$), the cohesion was weak and the values of S_f measured for the fine sand were lower than those measured for the coarse and medium sands.

In this study, and when comparing the data obtained for the Gebidem and Condit dams and for the laboratory experiments by [24], the efficacy of flushing, i.e., V_s / V_w , increases as V_w / h_s^3 decreases. This reveals that, although the volume of sediment evacuated from a reservoir increases as the volume of water increases, large increments in the volume of water only yield marginal increments in the volume of sediment evacuated. The higher values of efficacy registered for the Gebidem and Condit dams, and for the experiments by [24]

with respect to the results of this study, can be attributed to lateral erosion. This erosion, not registered in this study, contributed by increasing in the total amount of sediments evacuated for a given volume of water, which resulted in higher values of V_s/V_w . In these experiments, the efficacy of flushing increases as the initial bed slope increases (S_0), because steep bed slopes enhance the transport capacity of the flow. The effect of the sediment grain size (D^*) on the efficacy of flushing was limited to that related to the apparent cohesion for the fine sand. Thus, in those experiments with high values of h_s (low values of V_w/h_s^3), the efficacy of flushing measured for fine sand was lower than that measured for the coarse and the medium sands (Figure 6).

5. Conclusions

This study presents a comprehensive and systematic analysis of the effects of the initial volume of water, the initial water head, the bed slope, and the sediment grain size on the efficacy of flushing, when only the water previously stored in the reservoir is used. In addition, a group of dimensionless parameters have been derived to characterize this type of flushing. Nevertheless, the representativeness of the results obtained in this study is limited to those cases whose geometry, sediment characteristics, and initial conditions are within the range of values of the parameters tested in this study.

The results show that the volume of sediments evacuated from the reservoir increases as the initial volume of water and the bed slope increase. However, for relatively high initial volumes of water, only marginal increments in the volume of sediments evacuated were obtained. Thus, the efficacy of flushing, i.e., the ratio of the volume of sediments to the volume of water released, increases with the bed slope and decreases as the initial volume of water increases. These trends are corroborated by previous studies based on field observations and laboratory experiments. Nevertheless, owing to the absence of lateral erosion in these experiments, the values obtained in this study for the volume of sediments evacuated and for the efficacy of flushing are lower than those reported in previous studies, in which lateral erosion exists.

Regarding the sediment size, the results obtained for the fine sand differed from those obtained for the medium and coarse sands, owing to the existence of apparent cohesion in the sediment beds prepared with fine sand. The effect of this cohesion was significant in the experiment performed with relatively thick layers of fine sand, i.e., high values of h_s ; whereas for the experiments performed with relatively thin layers of fine sand, the effect of the apparent cohesion was negligible. Specifically, for a given volume of water, the apparent cohesion reduced the volume of sediment evacuated and hence, the efficacy of flushing, in comparison to those experiments performed with the medium and coarse sands. On the contrary, for those experiments performed with thin layers of fine sand, both the volume of sediment evacuated and the flushing efficacy were higher than those measured for the medium and coarse sands.

Author Contributions: All authors made a significant contribution to the research. S.G.-L. and J.A.T. performed the formal analysis of data and developed the methodology under the guidance and supervision of L.G.C. Results were thoroughly discussed by the three authors. All authors have read and agreed to the published version of the manuscript.

Funding: This study is part of the project EFISED (20403/SF/17) funded by the Fundación Séneca from Región de Murcia (Spain). The second author thanks the Escuela Politécnica Nacional (Ecuador), the Fundación Carolina (Spain), and Universidad Politécnica de Cartagena (Spain) for the financial aid received for his doctoral studies.

Institutional Review Board Statement: Not applicable.

Informed Consent Statement: Not applicable.

Data Availability Statement: The data presented in this study are available on request from the corresponding author. The data are not publicly available as they are part of broader ongoing research.

Conflicts of Interest: The authors declare no conflict of interest.

References

1. Annandale, G.W.; Morris, G.L.; Karki, P. *Extending the Life of Reservoirs: Sustainable Sediment Management for Dams and Run-of-River Hydropower*; The World Bank: Washington, DC, USA, 2016. [\[CrossRef\]](#)
2. Morris, G.L.; Fan, J. *Reservoir Sedimentation Handbook: Design and Management of Dams, Reservoirs, and Watersheds for Sustainable Use, 1.04*; McGraw-Hill Book Co.: New York, NY, USA, 1998.
3. Kondolf, G.M.; Rubin, Z.K.; Minear, J.T. Dams on the Mekong: Cumulative sediment starvation. *Water Resour. Res.* **2014**, *50*, 5158–5169. [\[CrossRef\]](#)
4. Franssen, N.R.; Tobler, M. Upstream effects of a reservoir on fish assemblages 45 years following impoundment. *J. Fish Biol.* **2013**, *82*, 1659–1670. [\[CrossRef\]](#) [\[PubMed\]](#)
5. Bellmore, R.J.; Duda, J.J.; Craig, L.S.; Greene, S.L.; Torgersen, C.E.; Collins, M.J.; Vittum, K. Status and trends of dam removal research in the United States. *Wiley Interdiscip. Rev. Water* **2017**, *4*, e1164. [\[CrossRef\]](#)
6. Schleiss, A.J.; Franca, M.J.; Juez, C.; De Cesare, G. Reservoir sedimentation. *J. Hydraul. Res.* **2016**, *54*, 595–614. [\[CrossRef\]](#)
7. Mahmood, K. *Reservoir Sedimentation: Impact, Extent, and Mitigation*; Technical Paper WTP71; The World Bank: Washington, DC, USA, 1987.
8. Sumi, T.; Okano, M.; Yasufumi, T. Reservoir sedimentation management with bypass tunnels in Japan. In Proceedings of the Ninth International Symposium on River Sedimentation, Yichang, China, 18–21 October 2004; pp. 1036–1043.
9. Minear, J.T.; Kondolf, G.M. Estimating reservoir sedimentation rates at large spatial and temporal scales: A case study of California. *Water Resour. Res.* **2009**, *45*, 1–8. [\[CrossRef\]](#)
10. Shrestha, B.; Babel, M.S.; Maskey, S.; van Griensven, A.; Uhlenbrook, S.; Green, A.; Akkharath, I. Impact of climate change on sediment yield in the Mekong River basin: A case study of the Nam Ou basin, Lao PDR. *Hydrol. Earth Syst. Sci.* **2013**, *17*, 1–20. [\[CrossRef\]](#)
11. Guillén-Ludeña, S.; Manso, P.; Schleiss, A. Multidecadal Sediment Balance Modelling of a Cascade of Alpine Reservoirs and Perspectives Based on Climate Warming. *Water* **2018**, *10*, 1759. [\[CrossRef\]](#)
12. Kondolf, G.M.; Gao, Y.; Annandale, G.W.; Morris, G.L.; Jiang, E.; Zhang, J.; Cao, Y.; Carling, P.; Fu, K.; Guo, Q.; et al. Sustainable sediment management in reservoirs and regulated rivers: Experiences from five continents. *Earth's Future* **2014**, *2*, 256–280. [\[CrossRef\]](#)
13. White, R. *Evacuation of Sediments from Reservoirs*; Thomas Telford Publishing: London, UK, 2001. [\[CrossRef\]](#)
14. Cantelli, A.; Paola, C.; Parker, G. Experiments on upstream-migrating erosional narrowing and widening of an incisional channel caused by dam removal. *Water Resour. Res.* **2004**, *40*, 1–12. [\[CrossRef\]](#)
15. Wilcox, A.C.; O'Connor, J.E.; Major, J.J. Rapid reservoir erosion, hyperconcentrated flow, and downstream deposition triggered by breaching of 38 m tall Condit Dam, White Salmon River, Washington. *J. Geophys. Res. Earth Surf.* **2014**, *119*, 1376–1394. [\[CrossRef\]](#)
16. Major, J.J.; O'Connor, J.E.; Podolak, C.J.; Keith, M.K.; Grant, G.E.; Spicer, K.R.; Pittman, S.; Bragg, H.M.; Wallick, J.R.; Tanner, D.Q.; et al. *Geomorphic Response of the Sandy River, Oregon, to Removal of Marmot Dam*; U.S. Geological Survey: Reston, VA, USA, 2012. [\[CrossRef\]](#)
17. Atkinson, E. *The Feasibility of Flushing Sediment from Reservoirs*; Report OD 137; HR Wallingford: Wallingford, UK, 1996.
18. Batuca, D.G.; Jordaan, J.M. *Silting and Desilting of Reservoirs*; Taylor & Francis: Oxfordshire, UK, 2000.
19. Di Silvio, G. Modeling Desiltation of Reservoirs by Bottom-Outlet Flushing. In *Movable Bed Physical Models*; Shen, H.W., Ed.; Springer: Dordrecht, The Netherlands, 1990; pp. 159–171. [\[CrossRef\]](#)
20. Castillo, L.G.; Carrillo, J.M.; Álvarez, M.A. Complementary Methods for Determining the Sedimentation and Flushing in a Reservoir. *J. Hydraul. Eng.* **2015**, *141*, 05015004. [\[CrossRef\]](#)
21. Dahal, S.; Crosato, A.; Omer, A.Y.A.; Lee, A.A. Validation of Model-Based Optimization of Reservoir Sediment Releases by Dam Removal. *J. Water Resour. Plan. Manag.* **2021**, *147*, 04021033. [\[CrossRef\]](#)
22. Esmaeili, T.; Sumi, T.; Kantoush, S.; Kubota, Y.; Haun, S.; Rütger, N. Three-Dimensional Numerical Study of Free-Flow Sediment Flushing to Increase the Flushing Efficiency: A Case-Study Reservoir in Japan. *Water* **2017**, *9*, 900. [\[CrossRef\]](#)
23. Esmaeili, T.; Sumi, T.; Kantoush, S.A.; Kubota, Y. Free-Flow Sediment Flushing: Insights from Prototype-Scale Studies. *J. Disaster Res.* **2018**, *13*, 677–690. [\[CrossRef\]](#)
24. Lai, J.-S.; Shen, H.W. Flushing sediment through reservoirs. *J. Hydraul. Res.* **1996**, *34*, 237–255. [\[CrossRef\]](#)
25. Shields, A. Application of similarity principles and turbulence research to bed-load movement. In *Hydrodynamics Laboratory Publ. No. 167*; Ott, W.P., van Uchelen, J.C., Eds.; U.S. Department of Agriculture, Soil Conservation Service Cooperative Laboratory, California Institute of Technology: Pasadena, CA, USA, 1936.
26. van Rijn, L.C. Sediment Transport, Part I: Bed Load Transport. *J. Hydraul. Eng.* **1984**, *110*, 1431–1456. [\[CrossRef\]](#)
27. Lai, J.-S. *Hydraulic Flushing for Reservoir Desiltation*; University of California, Berkeley: Berkeley, CA, USA, 1994.
28. Tullos, D.; Wang, H.-W. Morphological responses and sediment processes following a typhoon-induced dam failure, Dahan River, Taiwan. *Earth Surf. Process. Landf.* **2014**, *39*, 245–258. [\[CrossRef\]](#)
29. Begin, Z.B.; Schumm, S.A.; Meyer, D.F. Knickpoint Migration due to Baselevel Lowering. *J. Waterw. Port Coast. Ocean Div.* **1980**, *106*, 369–388. [\[CrossRef\]](#)
30. Brush, L.M.J.; Wolman, M.G. Knickpoint behavior in noncohesive material: A laboratory study. *GSA Bull.* **1960**, *71*, 59–74. [\[CrossRef\]](#)

31. Schumm, S.A.; Mosley, M.P.; Weaver, W.E. Incised Channels. In *Experimental Fluvial Geomorphology*; John Wiley & Sons, Ltd.: Hoboken, NJ, USA, 1987; pp. 192–225.
32. Loget, N.; Van Den Driessche, J. Wave train model for knickpoint migration. *Geomorphology* **2009**, *106*, 376–382. [[CrossRef](#)]
33. Shepherd, R.G.; Schumm, S.A. Experimental study of river incision: Discussion and reply. *Geol. Soc. Am. Bull.* **1976**, *87*, 320. [[CrossRef](#)]
34. Doyle, M.W.; Stanley, E.H.; Harbor, J.M. Geomorphic analogies for assessing probable channel response to dam removal. *J. Am. Water Resour. Assoc.* **2002**, *38*, 1567–1579. [[CrossRef](#)]
35. Pizzuto, J. Effects of dam removal on river form and process. *Bioscience* **2002**, *52*, 683–691. [[CrossRef](#)]
36. Doyle, M.W.; Stanley, E.H.; Harbor, J.M. Channel adjustments following two dam removals in Wisconsin. *Water Resour. Res.* **2003**, *39*, 1–15. [[CrossRef](#)]
37. MacBroom, J.G. Evolution of Channels Upstream of Dam Removal Sites. In *Proceedings of the Managing Watersheds for Human and Natural Impacts*, Williamsburg, VA, USA, 19–22 July 2005; pp. 1–12. [[CrossRef](#)]
38. Bento, A.M.; Amaral, S.; Viseu, T.; Cardoso, R.; Ferreira, R.M.L. Direct Estimate of the Breach Hydrograph of an Overtopped Earth Dam. *J. Hydraul. Eng.* **2017**, *143*, 06017004. [[CrossRef](#)]
39. Pickert, G.; Weitbrecht, V.; Bieberstein, A. Breaching of overtopped river embankments controlled by apparent cohesion. *J. Hydraul. Res.* **2011**, *49*, 143–156. [[CrossRef](#)]